

# Facile Synthesis, Fabrication, and Characterization of Mesoporous Nanoparticles as Efficient Drug Delivery Channels

Saima Noreen\*, Hira Munir\*, Haseeb Anwar\*\*

\*Department of Biochemistry and Biotechnology, University of Gujrat, Gujrat 50700, Pakistan

\*\*Department of Physiology, Faculty of Life Sciences, Government College University, Faisalabad, Pakistan

**Abstract-** Herein, the authors have presented a facile synthetic route of mesoporous nanoparticles (MSNs), and their structural characterization with their use to be an efficient drug delivery channel for diclofenac sodium. X-ray diffraction measurements (XRD), and Fourier transform infrared spectroscopy were used to track the alteration of the parent nanoparticles. By varying the quantity of co-solvent introduced to the sol-gel solution, the MSNs formed had the varied particle morphological characteristics of the microporosity has aided in the management of particle shape and structure. MSNs having an average diameter of 200 nm and dual pore channel sections featuring pore sizes of 1.3–2.6 and 4 nm were investigated as drug carriers. The impact of multimodal pore systems on the precise discharge of the experimental pharmaceutical diclofenac sodium was studied. The diclofenac-loaded MS nanoparticles were then studied for their drug release ability, which was altered owing to morphological variations. MSNs proved a dispersion of their drug release behavior showing a continual supply of the drug in vitro. The results showed that the diclofenac sodium release pattern proves discrete zones, which may be attributable to the corresponding porosity channel zones contained on the nanoparticles. The multifunctional pore channel networks handled the changes in drug concentration during the extended release through MSNs. The mesopore design and customizable surface of mesoporous silica nanoparticles enable the inclusion of a variety of therapeutic compounds and regulated distribution to specific areas.

**Index Terms-** Mesoporous nanoparticles, Diclofenac, SEM, XRD, Drug delivery

## I. INTRODUCTION

Nanotechnology advancements have discovered intriguing prospects for a variety of biological [1] and therapeutic activities [2], including pharmaceuticals administration [3], innovative diagnostics [4] therapeutic agents. Because nanoparticles are so microscopic, they can approach very near a biological target molecule [5]. Numerous delivery carriers based on diverse nanomaterials, including polysaccharides, microcapsules, lipid membranes, nanotubes, and nanorods, have been developed in the previous decade [6]. Nanoparticles have lately surfaced as promising options for delivering messages to their intended recipients [7]. Therapeutic chemicals are delivered

to the targeted areas in a standard drug delivery system [8]. The loaded drugs must be encapsulated within the nanoparticles to obtain the intended therapeutic response and to prevent hazardous side effects [9]. To increase the circulation time of therapeutic medications and to regulate high dose levels [10], an efficient drug delivery mechanism must be included in polymeric nanocarriers [11]. Natural polymeric carriers are often chosen candidates for targeted drug delivery systems because of their diverse natural features such as bioactivity, good biocompatibility, low cytotoxicity, and minimal immunologic qualities. Mesoporous nanoparticles are a special type of silica nanoparticles, known for their applications in various fields like biomedicine. nanoparticles having Nanopores are extremely useful for loading materials such as medicines [12]. For several drug delivery applications, site-specific drug distribution is a prerequisite, especially for therapeutic pharmaceuticals [13]. Owing to the existence of organic functional groups and their biomedical applications, this has all been ascribed to their size, stability, and easily changeable capability [14]. Administration of drugs, drug tailoring, gene translation, tissue regeneration, and cell monitoring are just a few of the areas where they've found useful [15]. Adjustment of the interface of the particles is required to optimize drug loading and additionally in vitro drug-releasing study, which also includes a wide variety of theragnostic treatments [16]. Many studies have shown whether mesoporous silica nanomaterials are useful in a variety of medicinal activities, such as drug administration application areas [17]. Numerous procedures are being used to reach this purpose, though nanoparticles, particularly mesoporous silica nanomaterials, have increasingly piqued researchers' interest nanoparticles have attracted features. Drug delivery systems including the nanoparticles can increase the efficacy of many drugs to a considerable level. Nanoparticles can enhance permeability by circulating in the bloodstream (Ramasamy et al., 2014). Many physical properties of nanoparticles like their pore surface area allow the high loading of a specific drug and other therapeutic agents (Trewyn, Slowing, Giri, Chen, & Lin, 2007). Another type of mesoporous silica nanoparticle known as the hollow mesoporous nanoparticles have many unique properties like low density and a specific surface area which can be the best choice for many drug delivery systems. They also have excellent mechanical stability and high biocompatibility. But there are some limitations in the preparation of hollow mesoporous silica nanoparticles because of high dispersion and shell thickness.

Sol-gel processing, chemical vapor depositing, and a variety of numerous additional hydrothermal procedures are implemented to make mesoporous silica nanomaterials [18]. Additional silica nanoparticles, such as hexagonal nanoparticles, can always be made with organic acids. Cationic surfactants are also used for the preparation of various nanoparticles. Cationic surfactants are used as templates in these preparations [19]. Mesoporous silica nanoparticles are very helpful for loading many types of therapeutic drugs including anticancer drugs concerning their size as well as charge properties and they release these drugs *in vitro* as well as *in vivo* in a very controlled manner. Cisplatin itself and variants are among the most commonly employed anticancer drugs in clinical contexts [20]. Small organic molecules, on the other side, cause kidney toxicity, illness, hearing issues, and persistent peripheral artery disease, which cause patients a great deal of pain [21]. Drug delivery systems with inactive tumor targeting characteristics are being designed to reduce the toxic effects of platinum drugs by enabling nano metal therapeutics to be administered to tumor types via penetration and persistence. *In vitro* and *in vivo* imaging of targeting cells in drug loading systems is a major issue [22]. To overcome this issue, nanoparticles with different physical properties have been prepared. To minimize *in vitro* cytotoxicity, heavy metals are typically used in the creation of nanomaterials for drug delivery systems [23].

Because of their high bioactivity, mesoporous nanoparticles are the ideal drug carriers for a wide range of medicines, even those that are insoluble in water [24]. Because of their distinctive physical features, they have sparked a great deal of attention throughout various nanocarriers [25]. The purpose of this investigation was to create novel diclofenac with a hydrolytic interaction. The goal of this composition is to lower the doses of medicine while increasing its therapeutic properties.

## II. IDENTIFY, RESEARCH AND COLLECT IDEA

The chemicals such as Cetyltrimethylammonium bromide (CTAB), tetraethylorthosilicate (TEOS), aqueous ammonia(25 % w/w), and 2-hydroxymethyl cellulose were employed during the present investigation. Deionized water was used as a solvent. Sigma-Aldrich supplied all the chemicals. CARLO ERBA supplied standard sodium hydroxide (2 M NaOH) formulations. Without more filtration, all the solvents were employed.

### A. Synthesis of Mesoporous Silica Nanoparticles:

Such Mesoporous Nanoparticles production was accomplished using previously disclosed technology [26]. The 5.2 grams of CTAB had been added to 200 g of de-ionized water and agitated to get a clear solution during the synthesis method. An ammonium solution (21grams, 25wt%) was then added to the resulting solution vigorously in a round bottom flask at 80°C. After stabilization of temperature 20grams of TEOS were added to the resulting suspension. It was then incubated for two hours at 100°C followed by the collection of MSNs as a result of centrifugation by washing with hot methanol. The obtained product was then placed in a furnace for calcination to be done at 550°C.

Scanning electron microscope (SEM) model Hitachi S-4800 and transmission electron microscope (TEM) model Tecnai G2 20 S-TWIN were used to examine the morphology of the produced

samples. A small quantity of material was dispersed in water for specimen preparation. For SEM examination, a thin coating of the homogeneous sample solution was placed on the reflecting surfaces of silicon wafers and evaporated to dryness. For TEM investigation, the sample was cast on a carbon-coated copper grid. Only the first five MSNs were further characterized based on electron microscopy data (a to d). The diclofenac sodium-loaded Mesoporous Silica Nanoparticles have been characterized by XRD analysis, SEM and UV-Vis spectra. TEM images were acquired using a JEOL 1200 EX instrument. The nanoparticles were dissolved in ethanol before being deposited over a carbon-coated copper grid covered with carbon-based sheets. The surface area structure characteristics were measured using nitrogen adsorption-desorption experiments at 77 K on a Scanning electron microscope ASAP 2020 V3.00 H device. The Barrett Joyner-Halenda (BJH) technique was used to calculate volume fraction and dimension. The material (approximately 50 mg) was purged under vacuum at 393 K for 12 hours before the adsorption procedure. A PANalyticalX'Pert MPD (Philips 1710) diffraction pattern was used to detect small-angle powdered X-ray scattering (sa-XRD). The Spectra were acquired using a Cu Ka (1 14 0.15418 nm) irradiation; the 2 $\theta$  scattering orientations in the span from 1 to 7 were recorded at a frequency of 0.5 deg min<sup>-1</sup>. In ethanol, dynamic scattering measurements were carried out using a Cordouan Technologies DL 135 Texture analyzer. The length and diameter were shown in intensity format. UV-vis absorption spectra were collected using a Hewlett-Packard 8453 Spectrophotometrically. A Molecular Probe (Oregon, USA) Spectramax 384-well spectrometer with a 1cm route length quartz cuvette having a fixed slit size of 2 nm was used to record UV-visible spectra at ambient temperature. A spectrometer was used to record the FTIR spectra. Overall FT-IR spectra of freshly synthesized MSNPs, functionalized MSNPs, and The only drug was recorded using a spectrometer [27].

### B. Drug Loading

The drug was loaded into synthetic MSNs using a previously published solvent depositing approach [28]. This process combined immersion and solvent evaporation. The drug (Diclofenac sodium) was diluted in acetone at a 20mg/ml ratio, and 5ml of this solution was combined with 50mg of MSNs to stir the resulting solution for 48 hours before drying in a vacuum for the elimination of the solvent to get the final product as drug-loaded MSNs. 0.5 mM diclofenac solution was prepared in 100 mM phosphate buffer buffers at pH 5–9 and incubated at room temperature for 3 days (15 °C). After that, cells were cultured for 72 hours (doxorubicin samples) or 96 hours with different drug solutions at doses ranging between 0.05 to 10. mM. Subsequently, MTT cell viability tests were used to determine the cytotoxicity of the drug solutions, and IC<sub>50</sub> was calculated using multiple models. The drug-loaded onto MSNs functionalized with a drug/CN weight ratio of 1:2, which ensures 100% drug adsorption, to determine drug release over time under varied circumstances. The samples were combined using 100 mM sodium phosphate buffer pH 5.5/7.4 or cellular growth medium (MEM, phenol red-free) and incubated at 37 °C for 24, 48, or 72 hours after being incubated overnight at 4 °C.

### C. Drug Delivery

Cell cultures were cultivated for 24 hours in 96-well plates and incubated at 2000 cells per well in a 200 mL culture medium. Increasing amounts of MSNA or MSNR having diclofenac sodium were added to the MCF-7 cell culture medium. Three days following treatment, an MTT test was performed to assess the drug delivery capabilities of the various batches. Cells were treated in media having 0.5 mg mL<sup>-1</sup> of MTT (3-(4, 5-

dimethylthiazol-2-yl)-2,5-diphenyltetrazolium bromide; Promega) for 4 hours. The precipitated crystals were dissolved in EtOH/DMSO (v/v) after the MTT/media solution was removed. The solution absorbance was measured at 540 nm using a microplate reader.

### III. RESULTS AND DISCUSSIONS

#### A. UV spectra

To calculate the band gap, absorption spectra were employed [29]. The material was absorbed in the near-infrared (IR) range, as seen by the spectrum. MSNPs absorbed the visible light in the 700 nm wavelength range due to indirect interband transitions (Figure 1). Because of their substantial excitation binding energies at ambient temperature, MSNPs have a characteristic peak centred at 350 nm (Figure 1) [30]. The graph clearly showed that the material absorbs visible light, making MSNs a suitable photocatalysts material.

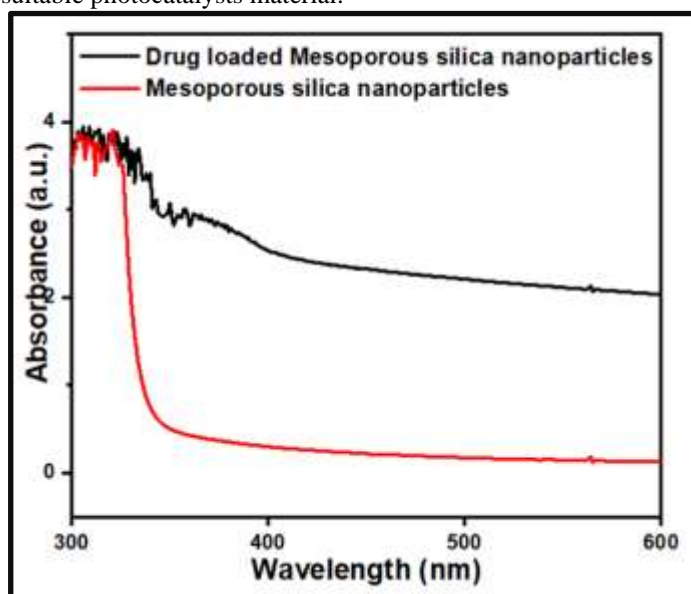


**Figure 1.** UV-visible analysis of drug-loaded MSNs

In addition, a wide band extends into the near-IR region. Some bands of the conduction and covalent band wave functions that contributed the based on the background have resulted in reduced NIR absorption. MSNs (red) absorbed a lot of light in the visible part of the Uv-vis spectra (422 nm). Throughout the visible range, MSNs-diclofenac sodium nanoparticles (black) also demonstrated a comparable absorption having a wavelength around 419.4 [31]. This provided that the drug was present within the nanospheres.

#### B. FT-IR analysis

Fourier Transform Infrared (FT-IR) analysis was carried out to determine the purity and origin of newly synthesized MSNs, as well as the availability of loaded drugs with them. Corresponding to silica peaks available in the literature, the frequency bands at 472, 809, and 1105 cm<sup>-1</sup> corresponded to the rocking vibration, symmetric stretching vibration, and asymmetric stretching vibration, respectively, of the Si-O-Si link. The Si-O-Si bond had about identical transmittance in the samples, showing that it was

stable following calcination. Furthermore, when the calcination temperature climbed, the adsorption band at 963 cm which corresponds to the bending vibration of the SiOH bond, diminished and eventually vanished at temperatures > 600 °C. The absorption bands at 1634 and 3442 cm<sup>-1</sup> were attributed to the twisting and stretching oscillations of the H-O-H bond, accordingly. The metal-oxygen (M-O) stretching and bending vibration were represented by the peaks at 450-510 cm<sup>-1</sup>. Metal oxides have absorption maxima in the range of 600 to 400 cm<sup>-1</sup> in general [32]. The M-O frequencies measured for the synthesized MSNPs were consistent with those reported in the literature. Significant spectral peaks in the FT-IR spectra of MSNs were found at 3456.0, 1632.3, 1485.2, and 1415.3 cm<sup>-1</sup>, respectively, corresponding to O-H stretching with hydrophobic interactions, N-H interacting of aromatic aldehydes, and C-C aliphatic stretch. Due to O-H stretching with hydrogen bonding [33], C-H stretch, -C=C- alkynes stretch and C-H bond, N-O symmetric stretch, and C-H vibrations, the FTIR spectra of MSNPs exhibited peaks at 3447.0, 3050., 2850, 2110, 1650, 1450, 1290, and 716.6 cm<sup>-1</sup>. Our drug-loaded FT-IR spectral analysis revealed distinct bands at 3580, 3440, and 3335 cm<sup>-1</sup>, corresponding to considerable O-H stretch, O-H stretching and H-bonded, C-H lengthening, C-C stretch across hydrocarbons, and C-O stretching pattern [21].

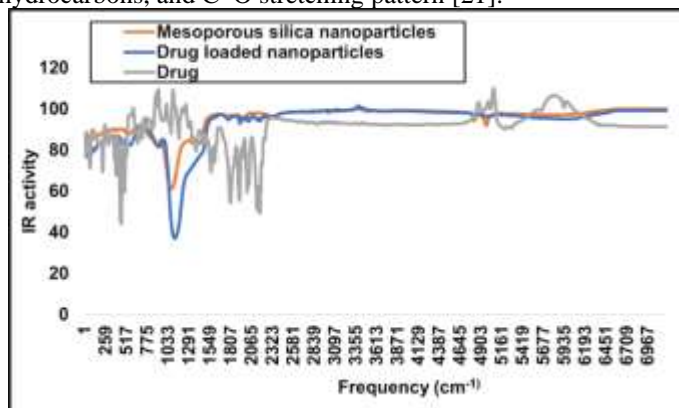


**Figure 2.** FT-IR spectra of newly synthesized MSNPs, drug-loaded MSNPs and the Only drug

#### C. Morphological parameters

The XRD fingerprint for the calcined MSNs is shown in Figure 3. All the diffraction characteristics were congruent with those available in the literature and may be ascribed to the hexagonal MSNPs [34]. Particles as small as 10–30 nm have been discovered [35] on the SEM images of MSNs thick layers over silica substrate. As can be seen, it has a porous structure that gives these particles a large surface area (Figure 3).

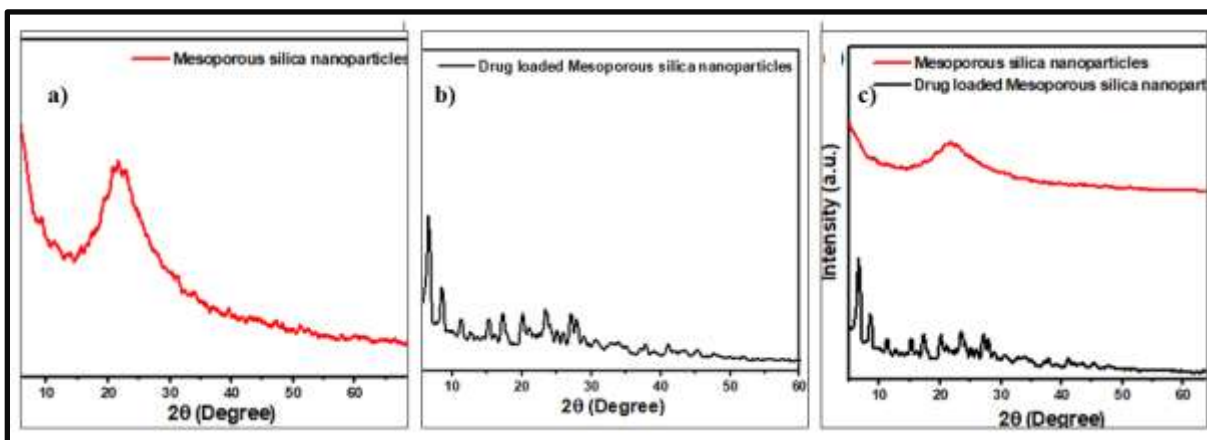


**Figure 3.** XRD analysis of (a) MSNs (b) drug-loaded MSNs and their (c) comparisons

The drug-loaded MSNs had a circular morphology with an average diameter of 200 to 300 nanometers. Despite pore passages running all through the interior of the nanoparticles, the ordered porosity structure was clear. Figure 4 shows a magnified TEM picture of a single particle (a). A boundary of around 15–25 nm is detected surrounding each particle, showing that the porosity channels are oriented differently at the perimeter than the centre microchannels, showing a dual microchannels form of facility. The findings of the investigation were consistent with previously reported data [36]. The nanoparticles had a strong inclination to combine, and larger aggregates developed very soon. At a pH of 7.2, the zeta potential was 17.3 mV, which is smaller than the value published for MSNs. The amount of adsorbent surface in a material (silica) influences its sensitivity, which is reflected by the zeta potential obtained by spectrometric investigation. Surface producing large quantities is particularly significant for drug loading because more surface functional groups can keep more drugs through secondary interaction with the oppositely charged groups on the drug. The mechanical homogeneity of the nanoparticles has been validated by elemental composition, which indicated only a trace of carbon (0.40%) and hydrogen (0.48%). It guaranteed that nanoparticles were made in such a way that they could passively reach the leaky tumor vascular (EPR effect). The DLS results (nanoparticles with aggregates) matched the average size of the drug. The polydispersity index rises as the concentration of polymers and drugs rises. When compared to empty nanoparticles, the data revealed that the homogeneity of drug-loaded nanoparticles diminishes.

Particle dimensions and morphologies are shown in SEM photos (Figure 4). MSNs with their honeycomb-like architecture were corroborated by TEM pictures that show constant hexagonal connection configurations. This was consistent with earlier study findings. MSN-1 produced spherical nanoparticles (NPs)

with a limited particle size range of 150 nm in mean size (Figure 4a). Figure 1d shows MSNPs with a consistent size dispersion of 5  $\mu$ m when the NaOH concentration was lowered to 3.8 mM. By raising the dosage of Sodium hydroxide to 7.6 mM and raising the quantity of water to 42.22 moles, 100 nm nanostructures were created (MSN-5) (Figure 4a). The use of 26.67 moles of water (MSN2) resulted in particles with a diameter of 200 nanometers (Figure 4b). The SEM image in Figure 1c shows aggregated nanoparticles of 900 nm after increasing the amount of NaOH to 14.0 mM and increasing the quantity of H<sub>2</sub>O to 26.67 moles.

Numerous nanoparticles conglomerated when the concentration of NaOH was increased with a corresponding increase in the quantity of solvent, while a few lesser spheres developed. Reduced TEOS concentrations to 13.54 mM (MSN-6) resulted in particle agglomeration and inadequate mesopore channels (Figure 1f and Figure 2f). Further studies demonstrated that increasing the concentration of TEOS (MSN-7) resulted in the development of microscopic greyish particles. After the carbonization process, attempts to halve the concentration of CTAB (MSN-8) resulted in a greyish product. Similarly, in high CTAB concentrations, the product did not precipitate. There was no siliceous substance when the water content was reduced to 10.55 moles. The low deposition of NaOH used only to achieve small limited size dispersion droplets suggested that the configuration of the morphological features tipping point stabilizer had to be kept in a specific ratio concerning countless distinctive reagents to attain higher nanospheres, such that, someone with a delineated diameter, limited size comprehensive network size dispersal, and slight or no agglomeration. Various strategies for controlling the particle size and agglomerate characteristics of nanoparticles during liquid-phase fabrication have indeed been published in the literature. By completely separating the reaction spaces, high dilution has been shown to regulate nucleus development and agglomeration.

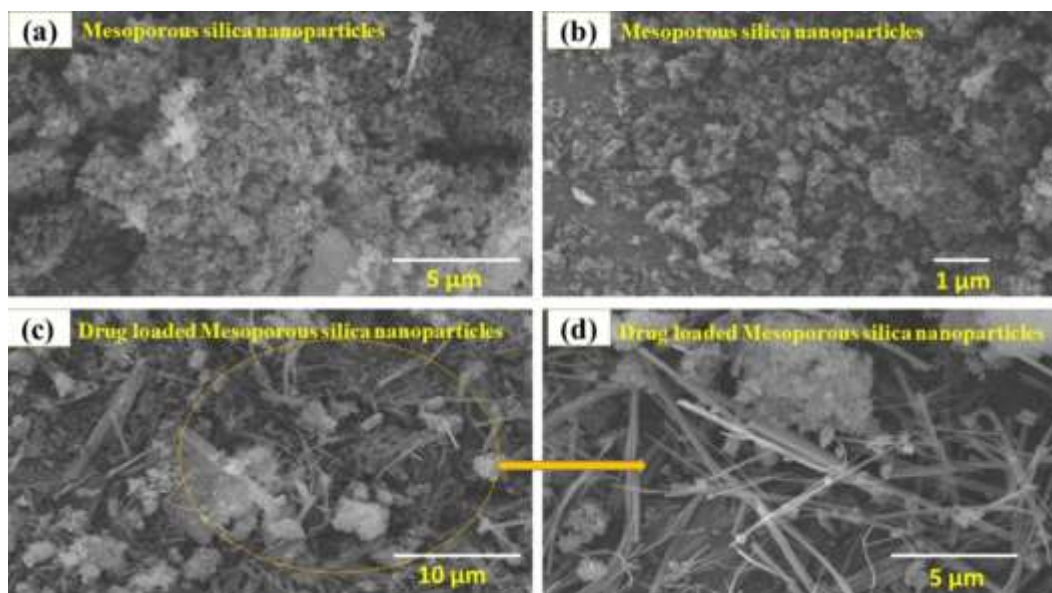


**Figure 4.** SEM analysis of (a) MSNPs@5µm (b) MSNPs@1µm (c) drug-loaded MSNPs@5µm and (d) drug loaded MSNPs@5µm

### C. Drug loading/delivery experiments

#### Drug loading

MSNs (10.3 mg) was initially distributed inside an Eppendorf tube having 1 gram of distilled water and 3.5 mg of doxorubicin. To promote penetration of a drug into the permeability, the dispersion was involved in incorporating for 5 minutes in a 318 K bath, then hydrochloric acid (0.02 M) was added to obtain pH 5.5. The scattering was then agitated for 24 hours at room temperature. The NPs were again recovered by centrifuged for 20 minutes. The loading capacity (wt%) was calculated as

$$\text{Loading capacity} = \frac{\text{Mass of Loaded Drug}}{\text{Mass of Drug loaded MSNs}} \times 100 \quad (1)$$

The first investigation sought to find the best pH and temperature settings for the medicine to load. It is usually recognized that diclofenac is hardly a good therapeutic drug in terms of analysis. Diclofenac sodium has been shown to self-associate in concentrated forms, is susceptible to photolytic degradation, and degrades at low pH. When refrigerated, it creates precipitates, that dissolve when returned to ambient temperature without loss of effectiveness. To sustain cell survival, drug delivery trials are typically done with a pH range of 5.5–7.5. However, we and others discovered that the adsorption of diclofenac to MSNPs functions better at higher pH, where the medicines are deprotonated. This suggests that a balance must be made between reaching best medication loading and preserving therapeutic efficacy.

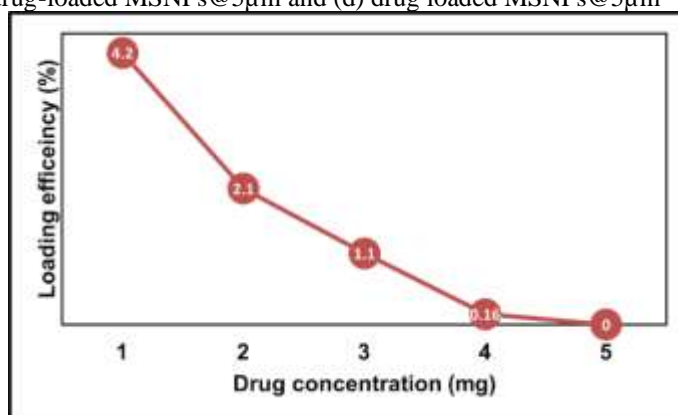


**Figure 5.** drug loading % as a function of concentration

We thus incubated these drug compounds for 3 days under a variety of pH ranges (5–9) and temperatures (4°C vs. 25°C) and then assessed their cytotoxicity using cell viability tests.

The pH effect on drug adsorption was then examined. Because of their intrinsic aromatic nature, diclofenac can adhere to the exterior of MSNP via p–p exchanges. Furthermore, both drugs include pH-sensitive substituents, making their interaction with MSNPs pH-dependent (enhanced at high pH and reduced at low pH). This could lead to medication release in acidic endocytic vesicles and the environment. MSNPs were grown with the drug at pH 5–9 for 18 hours, following which the samples were filtered and the amount of residual drug in the filtered solution was found using Uv-vis spectroscopy. Positive control lacked MSNPs and ranged in pH from 5 to 9. Figure 5 shows that, as predicted, diclofenac sodium bonded to nanoparticles more strongly as pH increased, with peak binding at pH 8–9. Most amino groups are dehydrogenated at these pH (pKa values between 8.3 and 8.6), rendering them more hydrophilic and susceptible to attaching to the nanotube surface via p–p contacts. In conjunction with the preceding experiment results, it can be inferred that a pH of 8 is ideal for doxorubicin attachment to MSNPs and a pH of 9 is optimum for diclofenac sodium adsorption, providing the binding procedure was conducted at 4°C in the darkness.

### Drug delivery

Following the development of MCM-41-type organized mesoporous silica (MS) by Mobil corporation researchers in 1992, there has been a lot of research into the controlled syntheses and applications of MSNs. Due to many distinguishing properties; they have been actively pushed as pharmaceutical delivery mechanisms since their development. Particle size distributions (F) calculated using the DLS approach, as well as TEM images of narrow size distribution MSNs with a particle diameter of 54 nm (A), 72 nm (B), 88 nm (C), 104 nm (D), and 188 nm (E). MSNs, that also involve the formulation of solid centre silica shell nanoparticles and successive full or partial withdrawal of the silica core; TEM images of hollow MSNs (B) and homogenous rattle type MSNs; MSNs, that also involve the formation of solid core/mesoporous silica shell nanoparticles and subsequent total or partial removal of the silica core.

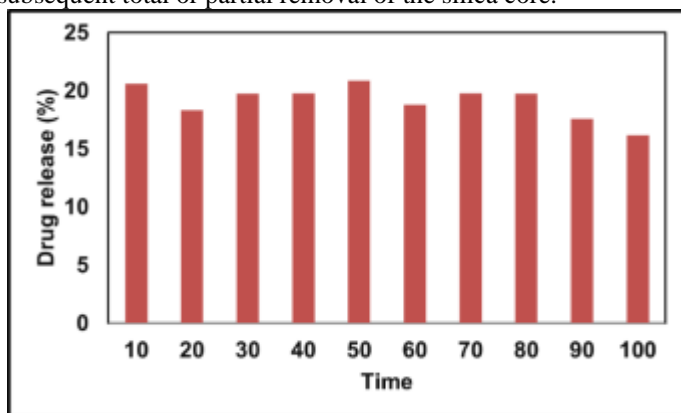


**Figure 6.** Drug release (%) as a function of time

Figure 6 depicts the impact of various PEG types on drug adsorption and dispersing stabilization. PEGylation decreased doxorubicin adherence by around 10%, but diclofenac interaction was very marginally reduced. The drug adsorption for each PEG component was quite comparable; however, only the MSNPs sample chemically modified with branching PEG (branched PEG 2500-NH<sub>2</sub>) remained stable, whereas the MSNPs had to precipitate out of solutions in all other instances. Based on the finding, we decided to conduct all future studies using branched PEG 2500-NH<sub>2</sub>. The aggregate molecular weight of the PEG molecules linked is 10 kDa (4 branches of 2.5 kDa each), which has previously been demonstrated to be ideal for the inhibition of nonspecific cellular uptake and beneficial regulatory genes.

**Table 1.** In vitro drug distribution over time (minutes), absorption, and absorption coefficient (%)

Time (Mints)	Absorbance	Percentage
10	0.205	20.5%
20	0.261	26.1%
30	0.288	28.8%
40	0.284	28.4%
50	0.211	21.1%
60	0.282	28.2%
70	0.296	29.6%
80	0.294	29.4%
90	0.291	29.1%
100	0.265	26.5%

\*The absorbance value is the average of three values. All experiments were conducted in triplicate.

Because of their amine functions, which make them hydrophilic at low pH and hydrophobic at high pH, diclofenac sodium should be released at low pH. We supported the drug delivery system for three days in buffers with pH 7.4 or 5.5 to validate this action at pH 5.5, which would be the equivalent pH the drug delivery mechanism would face in the receptor-mediated endocytosis channel. The samples were processed every 24 hours, and the released drug in the binding of diclofenac to MSNPs was measured at pH levels ranging from 5 to 9: the greater the pH, the stronger the drug interaction. UV/vis spectroscopy was used to measure the elute. The distribution of the drug had also been measured in cultured cells growth media (pH 7.4), which replicated the circumstances of a normal cell viability experiment. The medications were progressively released from their nanoparticle carrier at pH 5.5, as shown in Figure 6, with 44-55% of the drug liberated after 72 hours. In comparison, just 7% of the medication was released after the same period at pH 7.4. Furthermore, incubating the conjugates in cell growth media resulted in the considerable release of the drug: 23% of diclofenac after 72 hours. This indicated that during incubation, the linked drug was progressively dispersed on the nanotube exterior by cell culture medium constituents. The effect of the PEG category on drug receptor-associated and scattering consistency: only one PEG contender – branched PEG 2500-NH<sub>2</sub> – could promote a stable dispersion after the addition of the drug, so even though in all other situations, the nanotubes caused out of solution. In terms of the influence of density on drug adsorption and distribution stability, only the largest initial quantity of PEG added (5 mM) resulted in acceptable dispersion stability following drug addition, however this reduced drug interaction by around 40%. The values represented the nanoparticle-to-acidic-site ratio. This may allow for extracellular discharge of the medication from the nanoparticle carrier and subsequently diffusion across the cell membrane even without nanoparticles, but only for extended blood circulation durations.

### IV. CONCLUSION

This study suggests a potential approach for producing curcumin-loaded nanoparticles by microencapsulation utilizing CTAB (2.5%) and TEO (2%). This approach produced the mesoporous nanoparticles with particle sizes in the nanometer size (200–300 nm), which were employed *in vitro* drug delivery targeting diclofenac sodium as a drug sample. Particle Dimension Index (PDI) is used to calculate the average homogeneity of a particle solution, with higher PDI values indicating a wider size variation in the aggregate sample. PDI can also reflect nanoparticle clustering, as well as the uniformity and efficacy of particle surface changes across the samples. FT-IR spectra were implemented to evaluate calcined silica within the laboratory scale. With the rise in polymer and pharmacological concentrations, the PDI results from the Index value between 0.2-0.6 confirmed that the nanoparticles might have developed poly dispersive. The produced nanoparticles showed a circular morphology, including a diameter of 258 nanometers (Z average = 258 nm), according to the scanning electron microscope (SEM data). The medication interacts with the monomers through improved intermolecular interactions and engagement of carboxyl and aliphatic groups, according to FT-IR spectrum

measurements. Intermolecular chemical bonding also decreases phenolic oxygen intramolecular interaction. The auto-fluorescence feature of curcumin loaded in drug-MSNPs was shown using optical microscopy. Drug-MSNPs verified ( $\lambda_{\max} = 419.4$  nm) and PEGylated nano curcumin diclofenac sodium encapsulated in MSNPs ( $\lambda_{\max} = 650$ nm) by UV-Vis spectral analyses. As a result, drug loaded MSNPs might be a useful vehicle for delivering curcumin.

#### ACKNOWLEDGMENT

The authors are thankful to Higher Education Commission (HEC) of Pakistan for IRSIP tour to University of Glasgow, UK.

#### REFERENCES

- Sarikaya M, Tamerler C, Jen AK-Y, Schulten K, Baneyx F. Molecular biomimetics: nanotechnology through biology. *Nat Mater* 2003; 2:577–585.
- Bamrungsap S, Zhao Z, Chen T, Wang L, Li C, Fu T, Tan W. Nanotechnology in therapeutics: a focus on nanoparticles as a drug delivery system. *Nanomedicine* 2012; 7:1253–1271.
- Kumar A, Pandey AN, Jain SK. Nasal-nanotechnology: revolution for efficient therapeutics delivery. *Drug Deliv* 2016; 23:671–683.
- Rajitha B, Malla RR, Vadde R, Kasa P, Prasad GLV, Farran B, Kumari S, Pavitra E, Kamal MA, Raju GSR, others. Horizons of nanotechnology applications in female specific cancers. *Semin Cancer Biol* 2021; 69:376–390.
- Bai Y, Yang H, Yang W, Li Y, Sun C. Gold nanoparticles-mesoporous silica composite used as an enzyme immobilization matrix for amperometric glucose biosensor construction. *Sensors Actuators B Chem* 2007; 124:179–186.
- Mody V V, Cox A, Shah S, Singh A, Bevins W, Parihar H. Magnetic nanoparticle drug delivery systems for targeting tumor. *Appl Nanosci* 2014; 4:385–392.
- Williams J, Lansdown R, Sweitzer R, Romanowski M, LaBell R, Ramaswami R, Unger E. Nanoparticle drug delivery system for intravenous delivery of topoisomerase inhibitors. *J Control Release* 2003; 91:167–172.
- Yih TC, Al-Fandi M. Engineered nanoparticles as precise drug delivery systems. *J Cell Biochem* 2006; 97:1184–1190.
- He Q, Shi J. Mesoporous silica nanoparticle based nano drug delivery systems: synthesis, controlled drug release and delivery, pharmacokinetics and biocompatibility. *J Mater Chem* 2011; 21:5845–5855.
- Hassan AU, Sumrra SH, Imran M, Chohan ZH. New 3d Multifunctional Metal Chelates of Sulfonamide: Spectral, Vibrational, Molecular Modeling, DFT, Medicinal and In Silico Studies. *J Mol Struct* 2022; 132305.
- Mou X, Ali Z, Li S, He N. Applications of magnetic nanoparticles in targeted drug delivery system. *J Nanosci Nanotechnol* 2015; 15:54–62.
- Torney F, Trewyn BG, Lin VS-Y, Wang K. Mesoporous silica nanoparticles deliver DNA and chemicals into plants. *Nat Nanotechnol* 2007; 2:295–300.
- Popat A, Jambhrunkar S, Zhang J, Yang J, Zhang H, Meka A, Yu C. Programmable drug release using bioresponsive mesoporous silica nanoparticles for site-specific oral drug delivery. *Chem Commun* 2014; 50:5547–5550.
- Chakraborty I, Mascharak PK. Mesoporous silica materials and nanoparticles as carriers for controlled and site-specific delivery of gaseous signaling molecules. *Microporous Mesoporous Mater* 2016; 234:409–419.
- Tarn D, Ashley CE, Xue MIN, Carnes EC, Zink JI, Brinker CJ. Mesoporous silica nanoparticle nanocarriers: biofunctionality and biocompatibility. *Acc Chem Res* 2013; 46:792–801.
- Gohain MB, Pawar RR, Karki S, Hazarika A, Hazarika S, Ingole PG. Development of thin film nanocomposite membrane incorporated with mesoporous synthetic hectorite and MSH@ UiO-66-NH2 nanoparticles for efficient targeted feeds separation, and antibacterial performance. *J Memb Sci* 2020; 609:118212.
- Slowing II, Vivero-Escoto JL, Wu C-W, Lin VS-Y. Mesoporous silica nanoparticles as controlled release drug delivery and gene transfection carriers. *Adv Drug Deliv Rev* 2008; 60:1278–1288.
- Roig Sánchez S. Novel bacterial cellulose materials: Structuration, functional nanocomposites and photocurable hydrogels. 2021; .
- Moeller K, Kobler J, Bein T. Colloidal suspensions of nanometer-sized mesoporous silica. *Adv Funct Mater* 2007; 17:605–612.
- Sumrra SH, Hassan AU, Imran M, Khalid M, Mughal EU, Zafar MN, Tahir MN, Raza MA, Braga AAC. Synthesis, characterization, and biological screening of metal complexes of novel sulfonamide derivatives: Experimental and theoretical analysis of sulfonamide crystal. *Appl Organomet Chem* 2020; 34:.
- Hassan AU, Sumrra SH, Zafar MN, Nazar MF, Mughal EU, Zafar MN, Iqbal M. New organosulfur metallic compounds as potent drugs: synthesis, molecular modeling, spectral, antimicrobial, drug likeness and DFT analysis. *Mol Divers* 2021; .
- Sumrra SH, Hassan AU, Zafar MN, Shafqat SS, Mustafa G, Zafar MN, Zubair M, Imran M. Metal incorporated sulfonamides as promising multidrug targets: Combined enzyme inhibitory, antimicrobial, antioxidant and theoretical exploration. *J Mol Struct* 2022; 1250:131710.
- Takei K, Yu Z, Zheng M, Ota H, Takahashi T, Javey A. Highly sensitive electronic whiskers based on patterned carbon nanotube and silver nanoparticle composite films. *Proc Natl Acad Sci* 2014; 111:1703–1707.
- Zhang M, De Respinis M, Frei H. Time-resolved observations of water oxidation intermediates on a cobalt oxide nanoparticle catalyst. *Nat Chem* 2014; 6:362–367.
- Muhsan MS, Nadeem S, Hassan AU, Din AMU, Shahid S, Ali S. Synthesis of carbon nanoparticles by using seed oils. *Pakistan J Sci Ind Res Ser A Phys Sci* 2019; 62:1–7.
- Qiao Z-A, Zhang L, Guo M, Liu Y, Huo Q. Synthesis of mesoporous silica nanoparticles via controlled hydrolysis and condensation of silicon alkoxide. *Chem Mater* 2009; 21:3823–3829.
- Moballegheh Nasery M, Abadi B, Poormoghdam D, Zarrabi A, Keyhanvar P, Khanbabaee H, Ashrafizadeh M, Mohammadinejad R, Tavakol S, Sethi G. Curcumin delivery mediated by bio-based nanoparticles: a review. *Molecules* 2020; 25:689.
- Jiang H, Wang T, Wang L, Sun C, Jiang T, Cheng G, Wang S. Development of an amorphous mesoporous TiO2 nanosphere as a

- novel carrier for poorly water-soluble drugs: effect of different crystal forms of TiO<sub>2</sub> carriers on drug loading and release behaviors. *Microporous Mesoporous Mater* 2012; 153:124–130.
29. Hassan AU, Mohyuddin A, Nadeem S, Güleriyüz C, Hassan SU, Javed M, Muhsan MS. Structural and Electronic (Absorption and Fluorescence) Properties of a Stable Triplet Diphenylcarbene: A DFT Study. *J Fluoresc* 2022; .
30. Hassan AU, Sumrra SH, Raza MA, Zubair M, Zafar MN, Mughal EU, Nazar MF, Irfan A, Imran M, Assiri MA. Design, facile synthesis, spectroscopic characterization, and medicinal probing of metal-based new sulfonamide drugs: A theoretical and spectral study. *Appl Organomet Chem* no date; n/a:e6054.
31. Hassan AU, Mohyuddin A, Güleriyüz C, Nadeem S, Nkungli NK, Hassan SU, Javed M. Novel pull–push organic switches with D– $\pi$ –A structural designs: computational design of star shape organic materials. *Struct Chem* 2022; .
32. Hassan AU, Guleryuz C. THEORETICAL EVALUATION OF THE PERMEABILITY OF DISCHARGE ITEM (LiOOH) IN Li-O-2 BATTERIES. *Lat Am Appl Res* 2021; 51:153–157.
33. Hassan AU, Sumrra SH. Exploring the Bioactive Sites of New Sulfonamide Metal Chelates for Multi-Drug Resistance: An Experimental Versus Theoretical Design. *J Inorg Organomet Polym Mater* 2022; 32:513–535.
34. Wu KC-W, Yamauchi Y. Controlling physical features of mesoporous silica nanoparticles (MSNs) for emerging applications. *J Mater Chem* 2012; 22:1251–1256.
35. Bharde A, Kulkarni A, Rao M, Prabhune A, Sastry M. Bacterial enzyme mediated biosynthesis of gold nanoparticles. *J Nanosci Nanotechnol* 2007; 7:4369–4377.
36. Zhang J, Yuan Z-F, Wang Y, Chen W-H, Luo G-F, Cheng S-X, Zhuo R-X, Zhang X-Z. Multifunctional envelope-type mesoporous silica nanoparticles for tumor-triggered targeting drug delivery. *J Am Chem Soc* 2013; 135:5068–5073.

## AUTHORS

**Saima Noreen (MS)** –saimachaudhary463@gmail.

**Hira Munir (PhD)**

**Haseeb Anwar** –

**Correspondence Author** – Saimachaudhary462@gmail.com.